DOI: 10.13009/EUCASS2025-640
11TH EUROPEAN CONFERENCE FOR AERONAUTICS AND SPACE SCIENCES (EUCASS)

Investigation of the Laser-Aluminum Momentum Coupling Coefficient in the kHz-Regime for Laser Ablation Propulsion With Donut-Shaped Beam

Yoann LEVY[⋆†] *and Jaroslav HUYNH*[⋆] *and Martin CIMRMAN*[♮] *and Juraj SLÁDEK*[⋆] *and Jiří PACHMAN*[♯] *and Séverine A. E. BOYER*[°] *and Gilles TAHAN*[°,∇] *and Michel BOUSTIE*[Δ] *and Michel ARRIGONI*[◊] *and Martin SMRŽ*[⋆] and *Claude R. PHIPPS*[+] *and Stéphane ORIOL*[∇]

[⋆] *HiLASE Centre, FZU – Institute of Physics of the Czech Academy of Sciences, Dolní Břežany, Czech Republic*
[♮] *NTK Photonics, Zürich, Switzerland*
[♯] *Institute of Energetic Materials, Faculty of Chemical Technology, University of Pardubice, Czech Republic*
[°] *CNRS-CEMEF MINES Paris PSL, Sophia Antipolis, France*
[∇] *CNES, Paris, France*
[Δ] *CNRS-PPRIME, ISAE ENSMA, Poitiers, France*
[◊] *ENSTA Bretagne IRDL, Brest, France*
[+] *Photonic Associates, Santa Fee, USA*
[†] *yoann.levy@hilase.cz*

Abstract

In the context of laser ablation momentum transfer, we study the effect of a donut-shaped beam on the laser to momentum coupling coefficient for aluminum targets. The HiLASE Perla-B laser irradiations consisted in a train of 100 pulses with 1 kHz repetition rate, 1030 nm wavelength and a-few-picosecond pulse duration. To determine the coupling coefficient the targets are mounted on a ballistic pendulum placed in high vacuum and monitored by velocimetry. Comparison with Gaussian beam irradiation indicates that donut-shaped beams are less efficient for imparting momentum to Al targets in the regime of 10-20 Joules per squared centimeters.

1. Introduction

Only a few years after their invention, lasers were proposed for space propulsion. [1, 2] The key advantage lies in the ability to transfer energy over long distances (via ground, in-space optics, or space-borne lasers), allowing the spacecraft to be powered externally. This decouples the propulsion energy source from the vehicle, approaching an ideal scenario where propulsion duration is only limited by external resources. Laser-induced ablation propulsion, where recoil from ablated material generates thrust, was proposed early [3, 4]. Despite the energy required to vaporize material, laser ablation can transfer momentum efficiently with coupling coefficient of up to tens of kN per megawatt, far greater than the ~7 mN for pure photon (radiation) pressure. [5]

Consequently, laser ablation propulsion has emerged as a promising method, especially for addressing space debris remediation. [6, 7] The European Space Agency estimates over 141 million debris objects larger than 1 mm orbit Earth, [8] posing significant risks to missions, particularly in low Earth orbit. Global efforts aim to mitigate this threat, [9] and laser-induced momentum transfer could be a key solution provided the energy of the laser is well transferred into momentum of the target.

The efficiency of the momentum transferred is measured by the coupling coefficient, C_{m}, ratio of the momentum acquired by the irradiated target to the laser energy invested. It usually exhibits a maximum at an intensity between the threshold for the onset of ablation and the plasma regime. [9, 10] This maximum is of interest to obtain good efficiency of transfer. Therefore for each material and irradiation regime (fs-, ps- or ns- pulse durations, wavelength) it is important to characterize the coupling coefficient for different fluences and identify the optimum or ideal values.

In the field of laser processing beam shaping has gained interest for its ability to produce particular structures but also for some advantages related to the polarization symmetry they can offer [11–13]. Upon irradiation in the volume (for materials transparent to the laser wavelength) or of surfaces, it has been shown respectiveley that significant pressure waves can be generated [14] or that some micrometric ball of matter ejected [15, 16]. These aspects could

DOI: 10.13009/EUCASS2025-640

be beneficial to increase the laser-to-momentum coupling coefficient. Irradiations of a spherical flyer by ring-shaped beam has been also investigated in the frame of laser-ablation propulsion to assess the stabilization performance of the beam-shaping to keep the propelled target on track during the irradiation. [17, 18]

In this paper we report on tests of laser-momentum coupling of dounut-shaped beam on aluminum targets which is one of the prominent material used for space applications. We used the 1 kHz repetitive laser Perla-B [19] developed at HiLASE Centre (FZU – Institute of Physics of the Czech Academy of Sciences) with close to 2 ps pulse duration and 1030 nm wavelength. Preliminary results show about 25% lower efficiency in the coupling coefficient compared to Gaussian pulses of the same peak fluence in the regimes of irradiation between 10 and 20 J/cm^2.

2. Methods

The experimental setup employed is similar to that used in previous studies [20, 21] where the Al targets (1 mm thick) were fixed on a pendulum. The momentum generated by the laser ablation is directly transformed into kinetic energy of the pendulum, the pendulum movement monitored by photon Doppler velocimetry [22] (PDV) and the resulting electric signal analyzed to obtain the coupling coefficient.

A sketch of the setup is presented in Fig. 1. The Yb:YAG thin-disk laser Perla B [19, 23] provided 1030 nm wavelength pulses at 1 kHz repetition rate. The temporal profile of individual pulses was Gaussian with a duration of 2.8 ps full width at half maximum (FWHM). Each irradiation consisted in a train of 100 shots with 10 ms duration between them. The output spatial profile of the beam was Gaussian, slightly elliptical with a major and minor axis of 5.0 mm and 4.8 mm respectively. To create the donut-shaped beam (see inset in Fig. 1) from the Gaussian profile, a waveplate, based on birefringence-induced phase change, was introduced on the beam path.

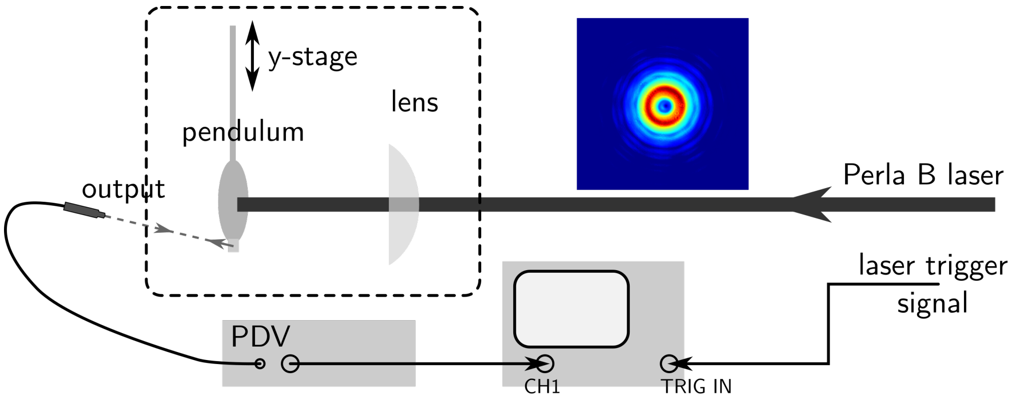

Figure 1: Set-up employed to irradiate the Al samples with Gaussian or donut-shaped beam and determination of the laser-ablation-induced momentum by the PDV

The donut-shaped beam was then focused with a plano-convex lens on an Al-target, both placed inside a vacuum chamber. The radius of donut-shaped beam peak fluence was $r_{\mathrm{max,D}} = (51\pm4)$ µm on the surface of the target determined by prior irradiations on smooth silicon sample mounted on the pendulum. The vacuum level in the chamber was never more than 3×10^{-4} mbar.

The holder of the pendulum was mounted on a motorized stage to allow vertical displacement of the target with respect to the constant laser height in the vacuum chamber. Thanks to the relatively small size of the laser spot on target and of the target damage, it was possible to make several burst irradiations, each on a fresh spot of the same Al by shifting the pendulum upwards by a few millimeters without breaking the vacuum. Accordingly, the PDV, also mounted on a displacement stage, was shifted upwards by the same amount.

The instantaneous frequency of the PDV electrical signal is directly proportional to the module of the velocity component of the pendulum in the direction of the PDV probe beam. To retrieve the velocity a post-processing in Python involving FFT algorithm was developed and applied to the signal with a running windows of width τ_{RW} of either 13 or 26 ms (for smaller signal amplitudes). The coupling coefficient, C_{m}, was retrieved from the pendulum velocity even in the presence of residual oscillations between the irradiations. A fit of the velocity over the duration of the laser action (100 ms) by a polynomial and its integration make it possible to retrieve the expression of the thrust Π imparted to the target and the C_{m} as $C_{\mathrm{m}} = \Pi/E_{\mathrm{p}}$.

DOI: 10.13009/EUCASS2025-640

3. Results and discussion

The analysis of the PDV signals enables one to calculate the coupling coefficients of the Al target for the train of 100 pulses and to evaluate the influence of the laser fluence and the laser beam shape. The Fig. 2 shows the results for donut-shaped beam irradiation for 5 different peak fluences on the target.

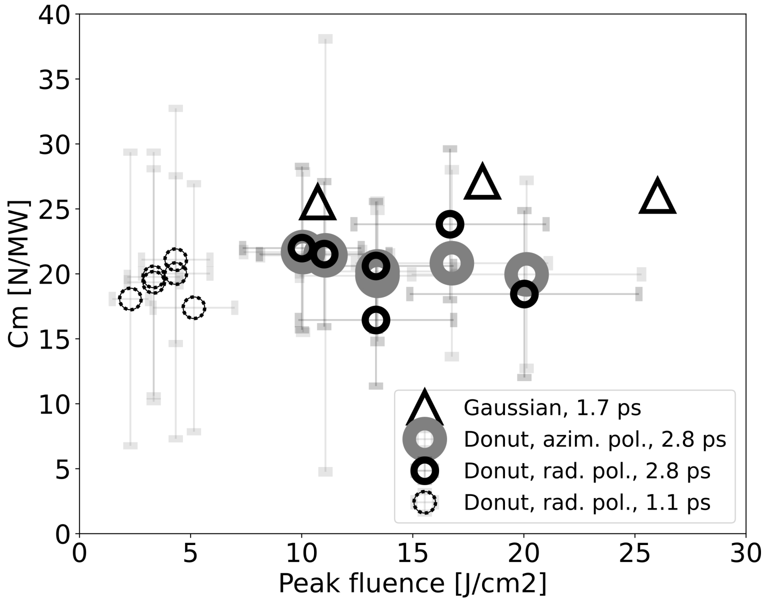

Figure 2: C_m coefficients obtained for picosecond, 1030 nm, Gaussian spatial profiles (triangles) and donut-shaped beams in radial (small black circles) or azimuthal (large thick grey circles) polarization states. Note the differences in the pulse durations of the laser employed, as indicated in the legend.

The C_m values are on the order of a few tens of N/MW in agreement with the literature related to near infrared irradiation of aluminum targets with pulse durations of 400 fs or 80 ps with similar fluences. [24] We have reported on the same graph the results obtained previously in similar experiment employing HiLASE PerlaB beamline [20] but with (1) Gaussian spatial profile, (2) larger characteristic spatial extension ($w_0 \sim 290\,\mu$m) and (3) although similar, slightly different pulse duration of 1.7 ps FWHM. For the regime of fluence (10 J/cm^2 - 20 J/cm^2) explored, the coupling coefficient with the donut-shaped beam reveals a lower efficiency compared to the Gaussian beam.

The Fig. 2 also shows the coupling coefficient obtained when considering two different polarization states of the donut-shaped beam, namely the radial and the azimuthal polarizations. Both give similar values.

To explore the regime of lower peak fluence that can be valuable to favor front side ejection of droplets of molten target (front side spallation) [16], and thus a possible increase in the momentum transfer, we have complemented the experiments on HiLASE PerlaB laser with a series of irradiation on a commercial, lower power, 1030 nm laser with 1.1 ps pulse duration FWHM and donut-shaped spatial profile with a radius $r_{max,D}$ of maximum fluence equal to $(43 \pm 7)\,\mu$m. The results are reported on the Fig. 2. The corresponding coupling coefficients are of the same order of magnitude as for the PerlaB series done with higher fluences (and larger pulse duration). Therefore, as a whole, over the regimes of peak fluence tested the efficiency of donut-shaped laser beams is reduced compared to that of a Gaussian beam.

Donut-shaped beams are subject to other disadvantages. Firstly, the energy to invest to reach a given ablation regime locally on the target is larger for a donut-shaped beam than that for a Gaussian spatial profile. Indeed, in a first approximation, neglecting heat conduction and laser-irradiation-induced stress waves, the local fluence on the target determines the regime of laser ablation at play [25] at that location and thus the main contribution to the thrust. It is thus interesting to compare the energy per pulse that is required to reach the same peak fluences with 2 different beam profiles (Fig. 3, left panel). In the case of a Gaussian beam shape, the radial distribution of fluence on the sample surface writes $F^{\text{Gauss}}(r) = F_0^{\text{Gauss}} \exp\left(-2r^2/w_0^2\right)$, where the peak fluence is reached along the optical axis ($r = 0$) and amounts $F_0^{\text{Gauss}} = 2E_p/(\pi w_0^2)$, with E_p the energy in the laser pulse and w_0 is the laser beam radius at 1/e^2 of intensity. In the case of a donut-shaped beam, the radial fluence distribution is given by $F^{\text{Donut}}(r) = 4E_p r^2/(\pi w^4) \exp\left(-2r^2/w^2\right)$, where w is a characteristic length of the spatial extension related to the radius $r_{max,D}$ of maximum fluence by $w = \sqrt{2}\, r_{max,D}$. Consequently, the peak fluence reads $F_0^{\text{Donut}} = 2E_p/(\pi w^2)\ e^{-1}$. For equal peak fluences between Gaussian and donut-

DOI: 10.13009/EUCASS2025-640

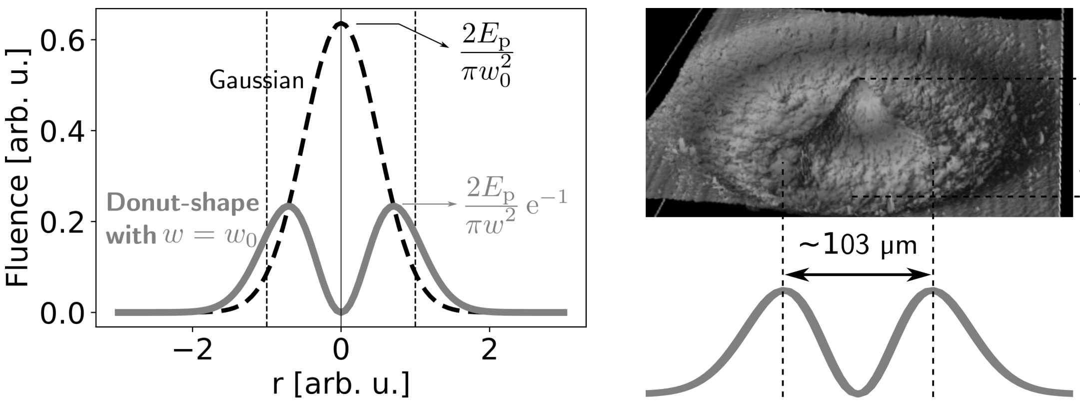

Figure 3: Left: comparison of the radial profile of fluence for a Gaussian (dashed black line) and a Donut-shaped beam (solid grey line) with the same energy per pulse and $w_0 = w$ materialized by the vertical dashed lines. Right: laser scanning confocal microscope reconstitution of the crater on Al resulting from the irradiation by a train of 100 pulses of the Perla-B beamline with 2.8 ps pulse duration.

shaped profiles, we therefore have $E_p^{Donut} = E_p^{Gauss} e^1 (w/w_0)^2$. For this reason, it should be borne in mind that, in spite of the fact that the C_m takes into account the energy invested, more energy per pulse (i.e. higher average power) is to be invested in the donut beam to reach a given peak fluence compared to Gaussian beam (when the characteristic dimensions of both profiles on target are similar).

Secondly, the damages induced by a donut-shaped laser beam are topographically more complex than those induced by Gaussian beams. As can be seen from the right panel in Fig. 3, the craters in the aluminum targets irradiated by donut-shaped beam exhibit a spike in the central part. The peak-to-valley amplitude is about 70 µm which may represent a source of roughness, perturbing the later irradiations (once the target has moved due to the propulsion) substantially more than in the case of a Gaussian beam. We note that the central protrusion in the right panel of Fig. 3 is extending beyond the original surface of the sample. It is not sure however whether a large central droplet of molten material have been ejected [15, 16] in our case or if it is solely due to the redeposition of the ablation products towards the center. [26] Further experimental studies involving fast camera imaging of the front size of the target should enable to clarify this point even though the regime does not seem attractive.

Finally, we point out that the different experiments carried out were not always focusing the beam with the same spatial extension on the target surface and we cannot exclude that the various spot sizes employed did not influence the efficiency of the laser to momentum coupling. In fact, the smaller the spot size, the more stress is expected [27] which plays a substantial role in the ablation mechanisms of materials upon irradiation by ultrashort laser pulses.

4. Conclusions

We have shown that upon irradiation by a train of 100 laser pulses at 1 kHz, with 2.8 ps duration and donut-shaped profile, the momentum transfer to an aluminum thick sample is about 25% less efficient compared to the case of Gaussian spatial profile with $\sim$ 1.7 ps, over a relatively limited range of peak fluences. Refinement towards medium fluences with constant pulse duration and similar spatial extensions are envisioned to confirm the trend. Additional future fast camera diagnostic, post-mortem analysis of the irradiation craters, possibly coupled with modeling of the laser-induced shock waves dynamics could bring insights into the possible conditions leading to front-side ejection of melt at the center of the beam that could be expected in the case of the donut-shaped profile to impart larger momentum without significant thermal losses.

5. Acknowledgments

This work was partly supported by European Union and the Ministry of Education Youth and Sports (MEYS) of the Czech Republic, Project SenDiSo: CZ.02.01.01/00/22_008/0004596, partly co-funded by European Union and the state budget of the Czech republic under the project LasApp CZ.02.01.01/00/22_008/0004573 and partly supported by CNES, the French space agency.

DOI: 10.13009/EUCASS2025-640

References

[1] F. B. Jr. Mead. Advanced propulsion concepts - project outgrowth. Technical report, Air Force Rocket Propulsion Laboratory, 1972.

[2] L. N. Myrabo. Advanced beamed-energy and field propulsion concepts. BDM corp. publication BDM/W-83-225-TR, final report, California Institute of Technology and Jet Propulsion Laboratory under NASA Contract NAS7-100, Task Order No. RE-156, 1983.

[3] G. A. Askar'yan and E. M. Moroz. Pressure on evaporation of matter in a radiation beam. *J. Exp. Theor. Phys.*, 16:1638, 1963.

[4] A. Kantrowitz. Propulsion to orbit by ground based lasers. *Aeronaut. Astronaut.*, 10:74–76, 1972.

[5] C. Phipps, M. Birkan, W. Bohn, H.-A. Eckel, H. Horisawa, T. Lippert, M. Michaelis, Y. Rezunkov, A. Sasoh, W. Schall, S. Scharring, and J. Sinko. Review: Laser-ablation propulsion. *J. Propul. Power*, 26(4):609–637, 2010.

[6] W. O. Schall. Orbital debris removal by laser radiation. *Acta Astronaut.*, 24:343–351, 1991.

[7] C. R. Phipps. L'ADROIT - a spaceborne ultraviolet laser system for space debris clearing. *Acta Astronaut.*, 104(1):243–255, 2014.

[8] ESA's Space Debris Office. Space debris by the numbers.

[9] B. Esmiller, C. Jacquelard, H.-A. Eckel, and E. Wnuk. Space debris removal by ground-based lasers: main conclusions of the european project CLEANSPACE. *Appl. Opt.*, 53(31):I45–I54, 2014.

[10] C. R., Jr. Phipps, T. P. Turner, R. F. Harrison, G. W. York, W. Z. Osborne, G. K. Anderson, X. F. Corlis, L. C. Haynes, H. S. Steele, K. C. Spicochi, and T. R. King. Impulse coupling to targets in vacuum by KrF, HF, and CO2 single-pulse lasers. *J. Appl. Phys.*, 64(3):1083–1096, 1988.

[11] M. Kraus, M. A. Ahmed, A. Michalowski, A. Voss, R. Weber, and T. Graf. Microdrilling in steel using ultrashort pulsed laser beams with radial and azimuthal polarization. *Optics Express*, 18(21):22305, 2010.

[12] T. Omatsu, K. Chujo, K. Miyamoto, M. Okida, K. Nakamura, N. Aoki, and R. Morita. Metal microneedle fabrication using twisted light with spin. *Opt. Express*, 18(17):17967–17973, 2010.

[13] K. K. Anoop, A. Rubano, R. Fittipaldi, X. Wang, D. Paparo, A. Vecchione, L. Marrucci, R. Bruzzese, and S. Amoruso. Femtosecond laser surface structuring of silicon using optical vortex beams generated by a q-plate. *Appl. Phys. Lett.*, 104(24):241604, 2014.

[14] V. P. Zhukov, A. M. Rubenchik, M. P. Fedoruk, and N. M. Bulgakova. Interaction of doughnut-shaped laser pulses with glasses. *J. Opt. Soc. Am. B*, 34(2):463–471, 2017.

[15] F. Takahashi, K. Miyamoto, H. Hidai, K. Yamane, R. Morita, and T. Omatsu. Picosecond optical vortex pulse illumination forms a monocrystalline silicon needle. *Sci. Rep.*, 6:21738, 2016.

[16] S. Syubaev, E. Mitsai, A. Porfirev, S. Khonina, S. Kudryashov, T. Katkus, S. Juodkazis, E. L. Gurevich, and A. Kuchmizhak. Silicon microprotrusions with tailored chirality enabled by direct femtosecond laser ablation. *Opt. Lett.*, 45(11):3050, 2020.

[17] D. T. Tran, C. Xie, and M. Koichi. Experimental investigations of impulse generation and stabilization performance on spherical target irradiated by donut-mode beam. In *48th AIAA Plasmadynamics and Lasers Conference*, 2017.

[18] D. T. Tran, C. Xie, K. Mori, A. Yogo, and H. Nishimura. Impulse generation and stabilization performance of a doughnut-spherical laser launch system. *J. Propul. Power*, 35(6):1057–1064, 2019.

[19] M. Smrž, J. Mužík, D. Štěpánková, H. Turčičová, O. Novák, M. Chyla, P. Hauschwitz, J. Brajer, J. Kubát, F. Todorov, and T. Mocek. Picosecond thin-disk laser platform perla for multi-beam micromachining. *OSA Continuum*, 4(3):940–952, 2021.

DOI: 10.13009/EUCASS2025-640

[20] G. Tahan. Laser ablation propulsion: experimental investigation on the influence of repetitive ablation. unpublished, 2023.

[21] S. A. E. Boyer, M. Schneider, M. Nour, M. Arrigoni, J. Le Clanche, M. Boustie, C. R. Phipps, Y. Levy, M. Divoky, J. Pilar, M. Hanus, P. Navratil, O. Denk, T. Paliesek, J. Pachman, S. Le Martelot, and S. Oriol. On the performance of high-power pulsed repeated laser irradiation for spatial structures propulsion. In Claude R. Phipps and Vitaly E. Gruzdev, editors, *High-Power Laser Ablation VIII*, volume PC12939, page PC129390T. International Society for Optics and Photonics, SPIE, 2024.

[22] J. Pachman, M. Künzel, O. Němec, and S. Bland. Characterization of Al plate acceleration by low power photonic Doppler velocimetry (PDV). In *40th International Pyrotechnics Society Seminar*, 2014.

[23] M. Chyla, T. Miura, M. Smrž, P. Severova, O. Novak, A. Endo, and T. Mocek. 50-mJ, 1-kHz Yb:YAG thin-disk regenerative amplifier with 969-nm pulsed pumping. In W. Andrew Clarkson and Ramesh K. Shori, editors, *Solid State Lasers XXIII: Technology and Devices*, volume 8959, page 89590S. International Society for Optics and Photonics, SPIE, 2014.

[24] C. R. Phipps, M. Boustie, J.-M. Chevalier, S. Baton, E. Brambrink, L. Berthe, M. Schneider, L. Videau, S. A. E. Boyer, and S. Scharring. Laser impulse coupling measurements at 400 fs and 80 ps using the LULI facility at 1057 nm wavelength. *J. Appl. Phys.*, 122(19):193103, 2017.

[25] M. V. Shugaev, M. He, Y. Levy, A. Mazzi, A. Miotello, N. M. Bulgakova, and L. V. Zhigilei. *Laser-Induced Thermal Processes: Heat Transfer, Generation of Stresses, Melting and Solidification, Vaporization, and Phase Explosion*, pages 1–81. Springer International Publishing, Cham, 2020.

[26] M. Zukerstein, J. Hrabovsky, J. Sladek, I. Mirza, Y. Levy, and N. M. Bulgakova. Formation of tubular structures and microneedles on silicon surface by doughnut-shaped ultrashort laser pulses. *Appl. Surf. Sci.*, 592:153228, 2022.

[27] Yiming Zhang, Benjamin Lauer, Beat Neuenschwander, and Valerio Romano. Numerical study of the influence of picosecond laser spot size on ablated depth and threshold fluence of metal. In Beat Neuenschwander, Stephan Roth, Costas P. Grigoropoulos, and Tetsuya Makimura, editors, *Laser Applications in Microelectronic and Optoelectronic Manufacturing (LAMOM) XXI*, volume 9735, page 97350M. International Society for Optics and Photonics, SPIE, 2016.